Title	Iridium Complexes Containing Mesoionic C Donors: Selective C(sp3)-H versus C(sp2)-H Bond Activation, Reactivity Towards Acids and Bases, and Catalytic Oxidation of Silanes and Water
Authors(s)	Petronilho, Ana; Woods, James A.; Müller-Bunz, Helge; Bernhard, Stefan; Albrecht, Martin
Publication date	2014-11-24
Publication information	Chemistry - A European Journal, 20 (48): 15775-15784
Publisher	Wiley
Item record/more information	http://hdl.handle.net/10197/6564
Publisher's statement	This is the author's version of the following article: Ana Petronilho, James A. Woods, Helge Mueller-Bunz, Stefan Bernhard, and Martin Albrecht, (2014) "Iridium Complexes Containing Mesoionic C Donors: Selective C(sp3)-H versus C(sp2)-H Bond Activation, Reactivity Towards Acids and Bases, and Catalytic Oxidation of Silanes and Water" Chemistry - A European Journal, 20(48) : 15775-15784 which has been published in final form at http://dx.doi.org/10.1002/chem.201404776
Publisher's version (DOI)	10.1002/chem.201404776

Iridium Complexes Containing Mesoionic C-Donors: Selective C(sp^3)–H *vs* C(sp^2)–H Bond Activation, Reactivity Towards Acids and Bases, and Catalytic Oxidation of Silanes and Water

Ana Petronilho,[†] James A. Woods,[‡] Helge Mueller-Bunz,[†] Stefan Bernhard,*[,‡] Martin Albrecht*[,†]

[†] *School of Chemistry & Chemical Biology, University College Dublin, Belfield, Dublin 4, Ireland*

[‡] *Department of Chemistry, Carnegie Mellon University, Pittsburgh, Pennsylvania 15213, United States*

E-mail: martin.albrecht@ucd.ie; bern@cmu.edu

Abstract

Metalation of the C2-methylated pyridylimidazolium salt **1** with $[IrCp^*Cl_2]_2$ affords either an ylidic complex **3** resulting from C(sp^3)–H bond activation of the C2-bound CH_3 group if the metallation is performed in the presence of a base such as AgO_2 or Na_2CO_3, or the mesoionic complex **4** via cyclometalation and thermally induced heterocyclic C(sp^2)–H bond activation, if the reaction is performed in the absence of a base. Similar cyclometalation and complex formation via C(sp^2)–H bond activation is observed when the heterocyclic ligand precursor consists of the analogous pyridyltriazolium salt **2**, *i.e.* when the metal bonding at the C2 position is blocked by a nitrogen rather than a methyl substituent. Despite the strongly mesoionic character of both the imidazolylidene in **4** and the triazolylidene in complex **5**, the former reacts rapidly with D^+ and undergoes isotope exchange at the heterocyclic C5 position, while the triazolylidene ligand is stable and only undergoes H/D exchange under basic conditions, where the imidazolylidene is essentially unreactive. The high stability of the Ir–C bond in aqueous solution over a broad pH range were exploited in catalytic water oxidation and silane oxidation. The catalytic hydrosilylation of ketones proceeds with turnover frequencies as high as 6,000 h^{-1} with both the imidazolylidene and the triazolylidene system, while water oxidation is enhanced by the stronger donor properties of the imidazol-4-ylidene ligands and is more than three times faster than with the triazolylidene analogue.

Keywords: carbene; mesoionic ligand; iridium; oxidation; stability

Introduction

Mesoionic/abnormal carbenes[1] have become attractive ligands in transition metal chemistry as they impart stronger donor ability[2] than Arduengo-type 2-imidazolylidenes.[3] These properties suggest that the incorporation of such mesoionic ligands can improve the catalytic activity, in parts due to the high electron density at the coordinated metal center and consequentially the accessibility of high-valent intermediates,[2] and in other parts because of the mesoionic character of the ligand, which offers potential for ligand participation in bond activation processes.[4] Recent work has indicated, however, that the stability of mesoionic carbene complexes may be limited.[5]

While the synthesis of the first mesoionic carbene complexes was rather serendipitous,[6] reliable methodologies have emerged during recent years for the selective preparation of mesionic complexes,[2] including, among others, the activation of the carbenic carbon,[7] the formation of free mesoionic carbenes,[8] and the steric protection[9] or chemical blocking[10] of more reactive positions. Specifically, introduction of substituents at the imidazolium C2 position of imidazolium salts has been successfully explored, even though control of chemoselective complex formation is not always achieved due to the non-inertness of some blocking groups and competitive metallation at the C4 or C5 position of the imidazole heterocycle.[11] Alternatively, the replacement of the C2 atom with a nitrogen atom to form a triazolylidene complex provides an easily accessible methodology for ligand synthesis based on click chemistry and for the formation of mesoionic carbene complexes.[12]

Here we report the synthesis of mesoionic carbene complexes derived from two structurally identical imidazolium and triazolium salts, **1** and **2** (Fig. 1), including methods for the selective activation of the exocyclic C(sp^3)–H bond or the C(sp^2)–H bond in the imidazolium precursor, stability aspects, and application as catalysts for hydrosilylation and water oxidation. Specifically, we provide evidence that the electronic character of isostructural mesoionic carbenes derived from imidazoles and triazoles are fundamentally different, and thus provide diverging opportunities for the design of novel active systems for catalysis and beyond.

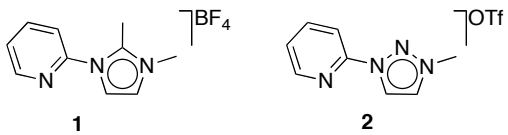

1 2

Figure 1. Isostructural ligand precursors for mesoionic carbene complexation.

Results and discussion

Reacting $[IrCp^*Cl_2]_2$ with the C2-methylated imidazolium salt **1** induces $C(sp^2)$–H or $C(sp^3)$–H bond activation. Thus, the ylidic complex **3** is selectively formed in the presence of Na_2CO_3 or Ag_2O, whereas $C(sp^2)$–H bond activation and formation of the abnormal/mesoionic carbene complex **4** is the exclusive pathway in the absence of a base and at elevated temperatures (100 ºC, toluene; Scheme 1).[13] While complex **3** was obtained in moderate yields (40%), complex **4** precipitated in solution upon formation as a yellow solid almost quantitatively (>85% yield).

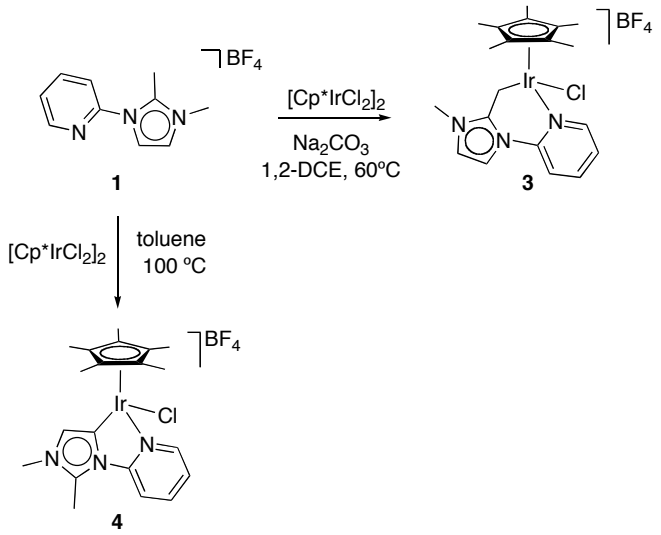

Scheme 1 Generation of complexes **3** and **4** from imidazolium salt **1**.

The formation of the ylide **3** instead of the abnormal carbene **4** in the presence of a base was previously observed for similar ligand systems and confirms the non-inertness of a methyl group at C2 as a protecting unit.[11] Due to the enhanced acidity of the C2-bound methyl group in the imidazolium salt **1**, formation of the corresponding abnormal carbene is inhibited under basic condition[14] and instead, the ylide complex **3** formed exclusively via $C(sp^3)$–H bond activation and no carbene complex was detected.

Spectroscopic analysis of both **3** and **4** enabled unambiguous characterization of both complexes. Complex **3** features a diagnostic AB doublet in the ^{1}H NMR spectrum, attributed to the Ir–CH_2 unit, at 3.45 ppm and 2.92 ppm**.** The two doublets of the CH_{imid} resonate at 7.95 ppm and 7.45 ppm, clearly showing that no aromatic metallation occurred. For complex **4,** a CH_{imid} singlet at 6.89 ppm and two CH_3 signals at 3.79 and 2.63 ppm, for the N–CH_3 and C–CH_3 units respectively, confirm the selective cyclometallation. In the ^{13}C NMR spectrum complex **3** shows a resonance at –2 ppm, which is diagnostic for an iridium-bound methylene

unit,[11b,13b] while the C–CH_3 signal is absent. In complex **4**, the signal assigned to the Ir–C_{imid} unit appears at 143.0 ppm, a value similar to that reported for related complexes.[10a]

Performing the reaction in the absence of a base cleanly yielded complex **4**, and thus provides a straightforward methodology for the synthesis of the abnormal carbene complex. The reaction is most likely comprised of an electrophilic C–H bond activation[15] via cyclometalation which is heteroatom-directed and hence thermodynamically controlled. The exclusive formation of **4** underlines the preference of $C(sp^2)$–H vs $C(sp^3)$–H bond activation and the formation of 5-membered metallacycles in cyclometallation processes.[16] Of note, heating of the thermodynamically presumably less stable ylide complex **3** in refluxing toluene for 48 h did not lead to any formation of complex **4**, indicating the absence of a low-energy isomerization pathway. This stability also suggests that $C(sp^2)$–H and $C(sp^3)$–H bond activation probably follow distinct reaction coordinates, in contrast to reactivity patterns established for related phosphine-functionalized imidazolium salts.[17] The base-assisted pathway leading to ylide complex **3** most likely involves only the methyl group and not the imidazole ring, which agrees with the successful isolation of the free ylide by Fürstner and coworkers.[14b] Moreover, calculations support the observed selectivity pattern of 2-methylimidazolium salts in the presence of a base, predicting that deprotonation of the heterocycle at C4/C5 is higher in energy than that of C2-bound CH_3 group by about 18 kcal mol^{-1}.[14e]

The triazolium salt **2**, a close analogue of the imidazolium salt **1**, reacted with the $[Cp^*IrCl_2]_2$ in toluene at elevated temperatures to produce the abnormal/mesoionic complex **5**, in analogy to the formation of complex **4** (Scheme 2). Attempts to use a transmetalation protocol via a silver carbene intermediate, a synthetic route commonly employed with triazolium salts,[12c] were less efficient, and the desired product was formed only in low yields which did not improve upon increasing reaction time or temperature. Instead mixtures of products were observed by ^1H NMR spectroscopy. The transmetalation procedure may be inefficient because the triazolium salt **2** contains two sites, C4 and C5, for metallation, and the corresponding silver carbene complexes presumably feature different stability properties and diverging carbene transfer rates. Attempts to isolate the silver carbene derivatives were not successful and the ligand was fully recovered.

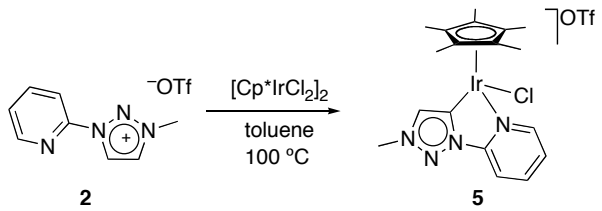

Scheme 2 Formation of complex **5** from triazolium salt **2**.

Complex **5** has been unambiguously characterized by NMR spectroscopy. The absence of one of the protons of the triazole ring at δ_H = 9.49 ppm and a new signal at δ_C = 155.5 ppm for the iridium-bound carbon suggest substitution of one proton at the triazolium heterocycle by a [IrCp*Cl] fragment. Moreover, pyridine coordination is indicated by the deshielding of the H_{pyr} resonances as compared to those in the ligand precursor **2**. It is worth noting that even upon lowering the reaction temperature, we did not succeed in detecting a *N,N*-bidentate coordinated nitrene complex[18] as a potential intermediate for a roll-over cyclometalation process,[19] as only starting materials were recovered under these conditions.

Attempts to form a nitrene complex via post-funtionalization of the triazole were also unsuccessful. Reaction of the 2-pyridyl-1-triazole **6** with the iridium precursor afforded complex **7** exclusively and no chelated product was observed (Scheme 3). Apparently, the high basicity of the triazole N3 compared to N2 compensates the stability gain associated with chelation.

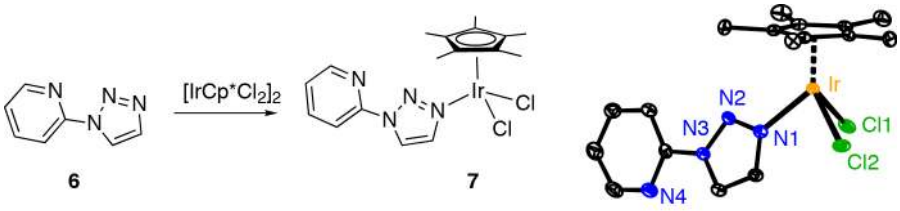

Scheme 3 Monodentate coordination of **6** to form complex **7**.

Complexes **3**–**5** were analyzed by X-ray diffraction analysis. Yellow crystals were obtained after slow evaporation of aqueous solutions of the complexes. The molecular structures confirmed the expected connectivity pattern inferred by NMR spectroscopy (Fig. 2). All complexes show the typical piano stool structure and a pseudo-tetrahedral coordination geometry around iridium (Table 1). The Ir–CH_2 bond in complex **3** is about 0.1 Å longer than the Ir–C_{imid} in complexes **4** and **5** (2.116(2) Å *vs* 2.004(7) and 2.019(5) Å, respectively) as expected for C(sp^2)–Ir *vs* C(sp^3)–Ir bonding.[13] Similarly, the ligand bite angle in the 6-membered metallacyclic complex **3** is some 4° larger than that of complexes **4** and **5**, featuring only a 5-membered metallacycle. The two heterocyclic rings in the ylide complex **3**

are mutually twisted by 27.5(3)º, while they are essentially coplanar in the pyridyl carbene complexes **4** and **5**.

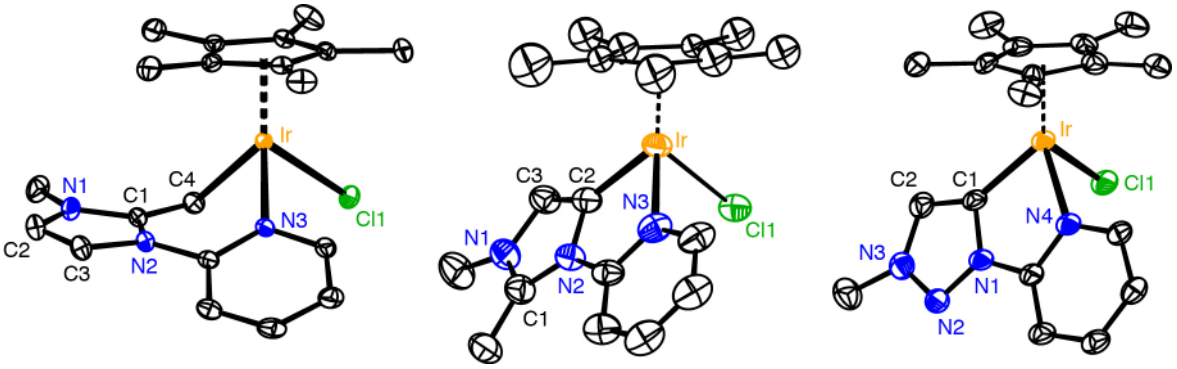

Figure 2 ORTEP plots for compounds **3**–**5** (50% probability, H atoms, non-coordinating anions and co-crystallized solvent molecules omitted for clarity). The Cp* ligand in complexes **4** and **5** is significantly disordered and only one position is shown.

Table 1. Selected bond lengths **(**Å**)** and angles **(º)** for the chloro complexes **3**–**5** and the aquo analogues **8**–**10**.

	3 [a]	**4** [a]	**5** [a]	**8** [b]	**9** [b]	**10** [b]
Ir(1)–C(1)	2.116(2)	2.004(7)	2.019(5)	2.1237(9)	2.025(2)	2.017(3)
Ir(1)–N(1)	2.121(2)	2.097(6)	2.110(4)	2.1242(7)	2.098(2)	2.127(3)
Ir(1)–X(1)	2.525(1)	2.4197(5)	2.4000(9)	2.16141(8)	2.156(2)	2.166(3)
C(1)–Ir(1)–N(1)	81.8 (1)	76.9(1)	77.7(2)	83.33(3)	77.11(8)	77.3(1)

[a] X = Cl; [b] X = O of OH_2

Abstraction of the chloro ligand in complexes **3**–**5** with AgOTf in aqueous CH_2Cl_2 afforded the dicationic aquo-derivatives **8**–**10**, respectively (Fig. 3). These complexes are highly water soluble, while the chloro precursors **3**–**5** required prolonged ultrasonication (1 h, 80 °C) to solubilize in aqueous media (1 μmol/mL). In addition, this ligand exchange provided access to a potentially labile coordination site for substrate coordination in catalytic applications. The ^{1}H NMR spectra of the aquo-complexes **8**–**10** are similar to those of the chloro analogues and are not significantly affected by the increased cationic nature of the metal center. The most diagnostic resonance pertains to the pyridinic α proton, which shifts slightly downfield (0.1–0.2 ppm) upon ligand exchange, possibly due to weak hydrogen bonding in the chloro species. Likewise the ^{13}C chemical shifts are essentially insensitive to the substitution and only minute shifts were observed.

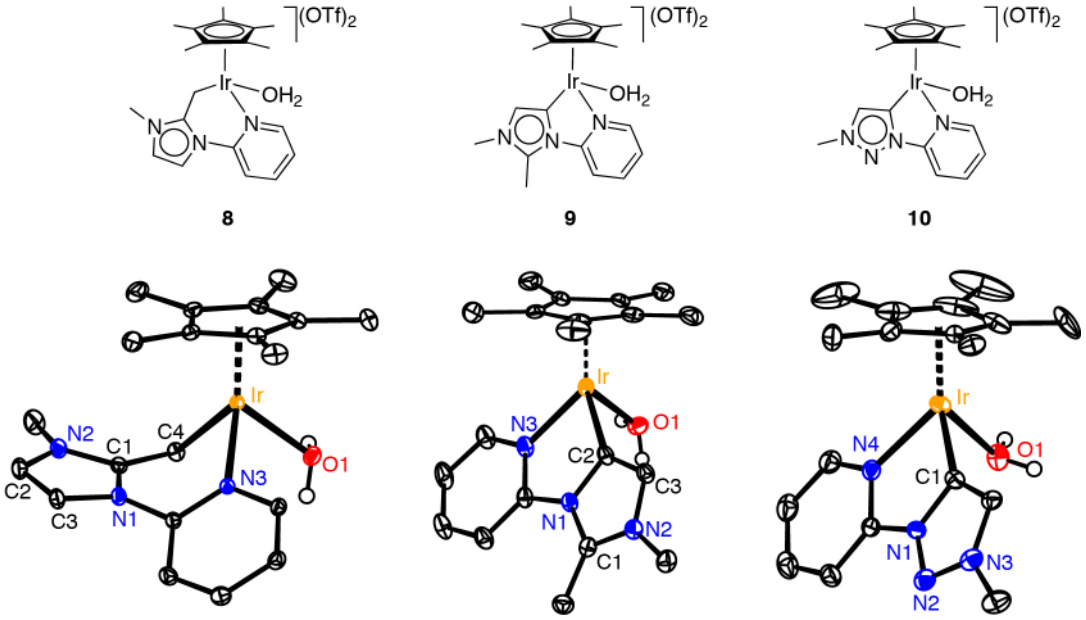

Figure 3 Schematic drawing and ORTEP plots for compounds **8**–**10** (50% probability, all H atoms except H_2O, non-coordinating anions and co-crystallized solvent molecules omitted for clarity). The Cp* ligand in complex **9** is disordered over two positions, only one of which is shown.

The structures of complexes **8–10** were confirmed by X-ray diffraction studies (Fig. 3) and the selective bond lengths and angles are summarized in Table 1. Complex **8** crystallizes with two molecules of water, one coordinated to the iridium center and the other located between the coordinated water and the triflate anion and stabilized by hydrogen bonding. The bond lengths between iridium and the *C,N*-bidentate chelate are identical within 3σ to the distances of the corresponding chloro complexes **3–5**, demonstrating a weak *cis*-influence of the ancillary ligand and remarkably little impact of the formal charge of the metal center.

Stability under acidic conditions. The persistence of these iridium complexes in an acidic environment was evaluated by ^{1}H NMR spectroscopic monitoring of complexes **3–5** in 1 M DCl (D_2O solutions). With all three complexes, no free ligand was detected in these experiments even when heated for 12 h to 80 ºC, which highlights the remarkable robustness of the Ir–$C_{carbene}$ bond and its resistance to harsh acidic conditions.[20,21] Longer heating resulted in slight decomposition of complex **3**,[22] while complexes **4** and **5** remain completely inert over several days. Microscopic stability was also indicated by the absence of any hydrogen/deuterium exchange in complexes **3** and **5** after several days. With complex **4** in contrast, selective incorporation of deuterium in the imidazole heterocycle is observed through disappearance of the H_{imid} resonance at δ_H = 7.00 ppm and concomitant appearance

of a signal at this frequency in the ^{2}H NMR spectrum (Scheme 4). Diagnostically, also the ^{13}C NMR resonance of the CH_{imid} carbon at δ_C = 121.8 ppm is absent in **4–D**.

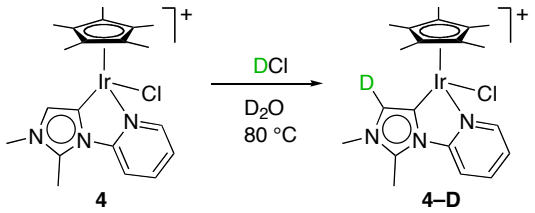

Scheme 4 Selective deuteration of **4** under acidic conditions.

The different behavior of **4** and **5** towards deuteration is worth noting. Only the imidazolylidene ligand in **4** is deuterated, while the triazolylidene in complex **5** is not, despite the fact that both complexes contain a mesoionic carbene ligand. Even when exposed to 3 M DCl at 80 °C for 48 h, complex **5** is recovered quantitatively and unmodified. This different reactivity may be associated with the lower aromaticity of imidazolylidene ligands as compared to triazolylidenes (resonance energies 22 and 26 kcal mol^{-1}, respectively).[23] This reduced aromaticity paired with a more pronounced anionic character in the imidazolylidene heterocycle, as inferred from the higher basic of the carbenic carbon, may facilitate the addition of a proton. The strongly mesoionic structure of the imidazolylidene ligand is thus surmised to promote dearomatization to yield intermediate **A**, resulting from protonation of a formal metallaallyl anionic fragment (Fig. 4).[24] In contrast, the additional nitrogen in the triazolylidene heterocycle, *viz* N2 instead of C2–CH_3, may act as a proton/deuterium scavenger and thus precludes H/D exchange at the heterocyclic carbon site (**B**, Fig. 4). Such Lewis-basic reactivity of N2 has been previously observed in catalytic systems using H^+ as an activator,[25] and in metal complexes revealing N2–metal coordination.[18] The effect may be reminiscent of the unusually high stability of platinum-bound bipyrimidines under strongly acidic conditions in the Catalytica system.[26]

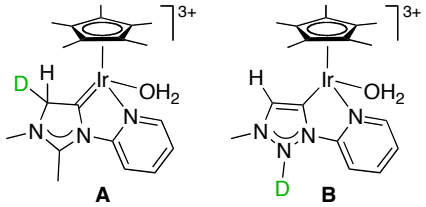

Figure 4 Proposed intermediates **A** and **B** resulting from deuteration of complexes **9** and **10**, respectively.

Stability under basic conditions. At high pH, the stability of complexes **3**, **4** and **5** is more limited than under acidic conditions, and all complexes gradually decompose when heated in

1M NaOH at 80 ºC for 24 h (D_2O solution). At room temperature, compounds **3–5** and **8–10** all form the corresponding iridium complex containing a hydroxide ligand, though the iridium–carbene bond is stable for several days. The complexes are all partly deuterated when dissolved in 1 M of NaOH in D_2O. Time-dependent ^1H NMR spectroscopy allows the sequence of deuteration to be monitored, thus providing access to selectivity patterns (Scheme 5).

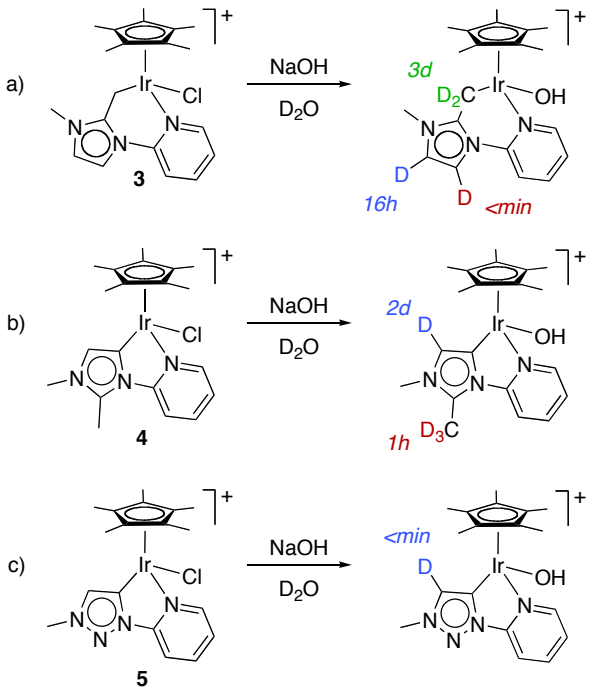

Scheme 5 Selective deuteration of **3–5** under basic conditions with times required for complete H/D exchange.

For compound **3** the deuteration of the imidazolylidene C5 carbon, *i.e.* the backbone site adjacent to the pyridyl substituent occurs immediately upon sample preparation, while the C4 carbon adjacent to the methyl substituents is completely deuterated only after 16 h. The CH_2 group undergoes H/D exchange as well, though the rate is substantially slower and complete deuterium incorporation requires about 3 days. The diverging rate of deuteration of the two C_{imid} sites is probably due to a combination of different acidity steric constraints. (*cf* X-ray structure, Fig. 1), The twist of the pyridyl and imidazole heterocycles facilitates access of the C5 position, while free rotation about the N–CH_3, may shields the C4 position to some extent. Complex **4** is fully deuterated at the C2-bound CH_3 group within 1 h, while deuteration of the heterocyclic carbon C4 is significantly slower and requires two days to reach completion. After deuteration of the imidazole ring, the compound is stable for several days but slowly decomposes to unidentified products upon heating. The same trend as in complex **4** was also

established for the imidazolium salt, where the acidity of the C–CH_3 group is higher than that of the CH_{imid} protons (*cf* metallation of **1** under basic conditions). Deuteration in the triazolylidene analogue of **4** takes places immediately upon sample preparation and involves the heterocyclic proton at C4 exclusively.

The different stability properties of these complexes in acidic and basic media suggest different mechanisms of deuteration. At high pH, a deprotonation/deuteration process is supported by the different rates of deuteration which reflect the acidity of the protons within the heterocycle and its substituents. In contrast, a deuteration/deprotonation mechanism is assumed under acidic conditions, which corresponds to local charge densities within the mesoionic rings (imidazolylidene > triazolylidene). Accordingly, the imidazolylidene in complex **4** is more nucleophilic (*cf* rapid H/D exchange under acidic conditions, very slow C_{imid} deuteration under basic conditions), while the triazolylidene ligand displays stronger electrophilic characteristics (*cf* fast H/D exchange with OD^-, no reaction towards D^+).

Catalytic water oxidation. The intrinsic activity of iridium(III) complexes in water oxidation[27] paired with the high stability of the Ir–C bond observed in particular in complexes **4** and **5** prompted us to investigate the performance of these complexes in water oxidation using cerium ammonium nitrate (CAN, 0.8 M) as sacrificial oxidant.[28,29] Oxygen evolution was monitored at different concentrations of iridium complex (Fig. 5) and reached in all cases the theoretical limit of oxygen production (2 mmol). This performance corresponds to a turnover number under dilute conditions (25 μM complex) of 8,000, comparing well with some of the most active systems known to date even though the conditions for **4** and **5** have not yet been optimized.[20,30] The oxygen evolution traces indicate about a twofold increase of catalytic activity when the mesoionic imidazolylidene is bound to iridium (complex **4**) as compared to the mesoionic triazolylidene analogue **5**. For example, the activity of a 50 μM solution of complex **4** is similar to that of a 100 μM solution of complex **5**. This higher activity may be directly associated with the higher electron density and the higher nucleophilicity of the imidazolylidene *vs* triazolylidene ligands (see also above). Stronger donor properties for imidazolylidenes have been reported previously,[12c,31] and hence, these ligands may provide easier access to high-valent intermediates that are crucial for water oxidation at a single metal site.[32]

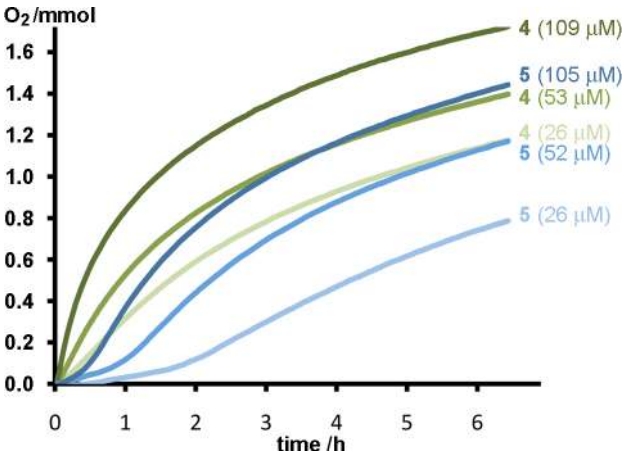

Figure 5 Oxygen evolution traces for complexes **4** and **5** at different concentrations, revealing significantly different initiation periods.

While the concentration dependence is unremarkable, however, catalytic runs with complex **5** feature a significant induction period in contrast to complex **4**. A plot of the turnover oxygen evolution rate over time further emphasizes this difference (Fig. 6). Complex **4** is immediately active and does not reveal any noticeable initiation period. The maximum oxygen evolution rate with this complex corresponds to a turnover frequency TOF = 0.4 s^{-1} , independent of the complex concentration. For complex **5**, the maximum TOF is about 0.2 s^{-1} (Table S1). These different activities and in particular the different initiation processes may point to a significantly different mechanism, or to a substantial advantage of strong donor 4-imidazolylidenes in mediating the rate-limiting step, presumably involving the access of a springloaded high valent iridium(V) oxo species. At later stages of the reaction, the oxygen evolution rates level off, which may be due to decreasing levels of Ce(IV) in the reaction medium, possibly inducing a change in mechanism.[33] Lowering of the more active catalyst concentration afforded turnover numbers in excess of 20,000 after prolonged reaction time, with no significant decrease of the oxygen evolution rates (Fig. S1). This activity suggests that much higher TONs may become accessible upon careful tailoring of the properties of the mesoionic C-donor ligand.

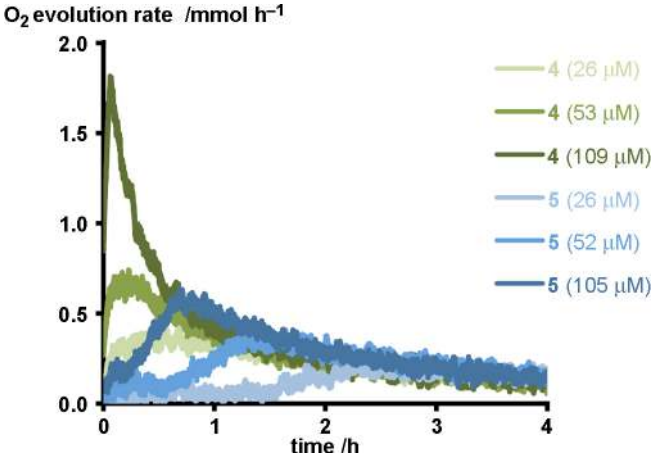

Figure 6 Time-dependent variation of oxygen evolution rates.

Catalytic hydrosilylation. The activity of complexes **8–10** as catalytic precursors for hydrosilylation of ketones was evaluated using the hydrosilylation of acetophenone as test reaction. In a typical reaction, acetophenone and triethylsilane were stirred in CD_2Cl_2 in the presence of the iridium catalyst to produce the silylether **II** (Table 2). Full conversions were achieved with all three complexes at 1 mol% loading (5 mM in iridium complex), while the corresponding chloro species **3–5** were inactive, suggesting that the availability of a labile solvento ligand is relevant for catalytic activity. Catalytic activity is resumed when complexes **3–5** where treated in situ with two equiv. AgOTf. Conversion under these conditions was incomplete after 30 min and according to ^{1}H NMR spectroscopy, the reaction was much less selective and a mixture of products was obtained. Probably the presence of two different metal centres provides access to alternative and competitive mechanisms and thus decreases the product selectivity. We did not observe any catalytic activity within 24 h when AgOTf was used in the absence of iridium complex under our standard conditions. Complexes **9** and **10** required less than 5 min to reach completion, whereas hydrosilylation with complex **8** is slightly slower (94% conversion after 5 min and full conversion after 30 min). The reaction is highly selective and the silylether is the only product formed from the ketone. Formation of the silylated enol ether was not detected with any of the complexes, in contrast to rhodium-catalyzed processes.[34] This catalytic activity is substantially higher than that reported for other NHC iridium complexes, which require longer reaction times (> 2 h) and additionally yield side products (> 5% silenol ether).[35] The activity of complexes **9** and **10** also compares favorably with Brookhart's PCP iridium complex, which achieves full conversion in about 20 min with 0.5 mol% catalyst loading.[36]

Table 2. Catalytic hydrosilylation activity of complexes **8–10** [a]

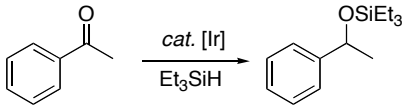

I **II**

entry	complex	loading	yield (5 min)	yield (15 min)	yield (2 h)	TON [b]	TOF_{50}
1	**8**	1%	>99%	--	--	100	>1200
2	**9**	1%	>99%	--	--	100	>1200
3	**10**	1%	>99%	--	--	100	>1200
4	**8**	0.1%	38%	50%	64%	810	2500
5	**9**	0.1%	47%	63%	93%	1000	6000
6	**10**	0.1%	40%	55%	86%	1000	2000
7	**8**	0.01%	6%	11%	14%	1400	--
8	**9**	0.01%	16%	20%	23%	2300	--
9	**10**	0.01%	4%	6%	13%	1600	--

[a] general conditions: acetophenone (0.5 mmol), iridium complex, Et_3SiH (1.0 mmol) CH_2Cl_2 (1.0 mL), RT; yields determined by ^1H NMR spectroscopy. [b] determined after 24 h.

Decreasing the relative catalyst loading to 0.1 mol% lowers the conversion rates and reveals differences in the catalytic activity of complexes **8–10**. Under these conditions, complex **9** is the fastest and accomplishes 47% conversion in 5 min and 90% conversion after 1 h, corresponding to a turnover frequency at 50% conversion, TOF_{50}, of about 6,000 h^{-1}. Complex **10** is significantly slower (TOF_{50} about 2,500 h^{-1}) and complex **8** displayed about three times lower activity with TOF_{50} ~2,000 h^{-1}. Moreover and in contrast to complexes **9** and **10**, this complex did not induce full conversion at 0.1 mol% loading even after extended reaction times. Of note, these runs were performed by increasing the substrate concentration rather than lowering the molarity of the complex. When catalytic reactions were performed with lower complex concentrations (0.5 instead of 5 mM) yet maintaining the 1000:1 substrate/complex ratio initial conversions were similar but rates dropped at later reaction stages when compared to the runs with 5 mM complex concentrations and activity eventually ceased before reaching full conversion (5 h, 74%). This outcome is independent of the quality of the CH_2Cl_2 used to prepare the iridium stock solution and to run the catalytic reaction (reagent grade *vs* freshly distilled from alumina/catalyst column system).

Further lowering of the iridium loading to 0.01 mol% required the lowering of the iridium complex concentration and was significantly less productive and catalytic activity ceased after about 2 h (14–23% conversion, Fig. S2), suggesting catalyst decomposition. Possibly, degradation is induced by minor impurities in the solvent or the reagents that become relevant at such low catalyst concentrations as observed with catalytic runs under dilute iridium concentrations (see above). It is tempting to attribute the different catalytic activities of complexes **8–10** to the donor properties of the mesoionic C-donor ligands, which is assumed

to increase from **8** < **10** < **9**. This sequence mirrors the catalytic activity of the complexes and might thus imply a rate-limiting step that involves either oxidative silane addition or product release, *i.e.* steps that would directly benefit from high electron density at the iridium center. While monitoring of the reaction mixture has been inconclusive, we noted the formation of a persistent hydride species, presumably formed upon reaction of the hydroxo or alkoxo ligand with the silane. These hydride species showed an NMR resonance at δ_H –14.00, –14.29 and –14.28 ppm for intermediates derived from complexes **8**, **9** and **10**, respectively. Only a single hydride species was apparent from complexes **9** and **10**, though complex **8** gave rise to several minor species with hydride resonances between –13.5 and –16 ppm. This less selective hydride formation may be correlated with the lower catalytic activity and incomplete conversions observed in catalytic runs and hint to undesired complex transformations under catalytic conditions.

Substoichiometric experiments using deuterium-labeled Et_3SiD as silylating agent did not induce any detectable deuterium incorporation into the heterocycle when using complexes **9** or **10** as catalyst precursors, suggesting that a cooperative interaction of the mesoionic C-donor ligand and the metal center does not play a critical role in the Si–H/D bond activation process.[24b]

Oxidation of Silanes. In all catalytic runs, vigorous hydrogen evolution was observed upon addition of the silylating agent, and H_2 formation was confirmed by the diagnostic singlet observed at δ_H 4.62 ppm in the ^{1}H NMR spectrum. Generation of H_2 is often associated with the formation of a silylenolether in ketone hydrosilylation reactions, however this side product was not observed with complexes **8**–**10**, and thus, hydrogen production most likely occurs through a different process. When using Et_3SiH, indeed formation of silanol and disiloxane was detected by the characteristic signals, similar to carbene rhodium-catalyzed oxidation of silanes.[24b] Silane oxidation is much faster and hydrogen formation more vigorous when using Ph_2SiH_2, and hence this silylating agent has been used for evaluating silane oxidation with complex **10** (0.5% catalyst loading). Upon addition of the diphenylsilane, hydrogen evolution starts instantaneously. In the NMR spectrum, several well-resolved aromatic signals were observed between 7.56 and 7.24 ppm, while the Si–H signal at 4.91 ppm was smaller and gradually disappeared. The transformation of the silane is complete after 6 h. At this stage, the aromatic region featured a complicated set of multiplets in the 7.81–7.23 ppm range. Formation of a yellow oil and an off-white crystalline precipitate was indicative for the formation of polymerized material. The crystalline solid was poorly

soluble in CH_2Cl_2 and $CDCl_3$ and thus easily separated from the oil. Its spectroscopic properties (^1H ^{13}C ^{29}Si NMR; IR), MS, and X-ray data are identical with previously reported data for $Ph_2Si(OH)_2$,[37] thus indicating the oxidation of the silane to the silane diol. The yellow oil displays a more complex set of signals in the NMR spectra, including broad and superimposed multiplets in the aromatic area and a several ^{29}Si NMR resonances between 28 and 34 ppm and beteen –48 and –60 ppm, consistent with the formation of oligo- or polymeric siloxanes.[38] Mass spectrometric analyses show a range of ions with low molecular weight (<1000 amu) with a repetitive unit of 198 amu corresponding to the Ph_2SiO monomer unit and hence suggest the presence of significant quantities of a poorly defined mixture of oligomeric siloxanes.

Conclusions

Iridium abnormal carbenes are easily generated by C–H activation and cyclometalation from the corresponding salt precursors. Selectivity over exocyclic $C(sp^3)$–H *vs* $C(sp^2)$–H bond activation in the 2-methylated imidazolium salt is achieved by applying either a base-mediated metalation or a cyclometalation methodology. The formed mesoionic complexes reveal a remarkably high stability towards acidic and basic aqueous media. While an abnormal carbene bonding mode is obtained both with triazolium and imidazolium precursor salts, the corresponding mesoionic C-donor ligands exhibit complementary reactivity patterns. According to H/D exchange experiments, the triazolylidene ligand is electrophilic, while the 4-imidazolylidene system is nucleophilic, thus indicating that the abnormal bonding mode can lead to most diverging reactivity patterns. In catalytic hydrosilylation of ketones, however, both carbene-type ligands induce a high activity and also allow for the polymerization of dihydrosilanes under mild conditions. Further work is directed towards the expansion of this oxidative coupling chemistry.

Experimental section

General. All reactions were performed under an atmosphere of dry dinitrogen in oven-dried glassware. All solvents used in the metallation reactions were purified using an alumina/catalyst column system (Thermovac Co.). 1-(2-pyridyl)-1,2,3-triazole (**6**) was synthesized according to literature procedures.[39] All other reagents are commercially available and were used as received. Unless specified otherwise, NMR spectra were recorded at 25 °C on Varian Innova spectrometers operating at 300, 400 or 500 MHz (^1H NMR) and

75, 100 or 125 MHz ($^{13}C\{^1H\}$ NMR), respectively, and at 80 MHz (^{29}Si NMR). Chemical shifts (δ in ppm, coupling constants J in Hz) were referenced to residual solvent resonances or $SiMe_4$. Assignments are based on homo- and heteronuclear shift correlation spectroscopy. Elemental analyses were performed by the Microanalytical Laboratory at University College Dublin, Ireland, by using an Exeter Analytical CE-440 Elemental Analyzer.

Compound 1. 2-methyl imidazole (3.28 g, 40 mmol), CuI (760 mg, 4.0 mmol) and KOH (6.74 g, 0.12 mol) were grinded and mixed with DMSO (20 mL). The mixture was heated at 50 °C for 1 h, then 2-bromopyridine (3.8 mL, 40 mmol) was added and the mixture was heated for 16 h at 130 °C. After cooling, the crude mixture was extracted with CH_2Cl_2 (2 × 250 mL) and the combined organic layers were washed with NaOH (1 M, 3 × 100 mL). The organic layer was collected, dried over $MgSO_4$, filtered and the solvent was removed under reduced pressure. The residue was dissolved in MeCN (15 mL) and reacted with MeI (40 mmol, 2.5 mL) in a microwave reactor (100 °C, 2 h). The resulting mixture was layered with Et_2O, and a white precipitate immediately formed. This solid was filtered off and dissolved in water (5 mL) and NH_4BF_4 was added (10 mmol, 1.0 g). The resulting mixture was stirred for 2 h and the solvent was removed under reduced pressure. The residue was suspended in CH_2Cl_2 (100 mL) and filtered. The solvent was removed under reduced pressure yielding compound **1** (3.75 g, 36%) as a white powder. ^1H NMR (400 MHz, $CDCl_3$): δ 8.61 (ddd, $^3J_{HH}$ = 4.7 Hz, $^4J_{HH}$ = 1.9 Hz, $^5J_{HH}$ = 1.0 Hz, 1H, H_{py}), 8.13–8.04 (m, 2H, H_{py}), 7.71, 7.64 (2 × d, $^3J_{HH}$ = 1.4 Hz, 1H, H_{imid}) 7.56 (ddd, $^3J_{HH}$ = 7.1 Hz, $^3J_{HH}$ = 4.7 Hz, $^4J_{HH}$ = 1.0 Hz, 1H, H_{py}), 4.09 (s, 3H, NCH_3), 2.94 (s, 3H, C–CH_3). $^{13}C\{^1H\}$ NMR (100 MHz, $CDCl_3$): δ 149.6 (CH_{py}), 147.5 (C_{py}), 145.0 (C_{imid}), 140.3 (CH_{py}), 125.7 (CH_{py}), 123.3 (CH_{imid}), 120.9 (CH_{imid}), 120.8 (CH_{py}), 36.9 (N–CH_3), 13.2 (C–*C*H_3). Anal. calcd. for $C_{10}H_{12}N_3BF_4$ (261.03) × $0.5H_2O$: C, 44.98; H, 4.78; N, 15.74. Found: C, 44.75; H, 4.39; N, 15.39. HRMS for $C_{10}H_{12}N_3$ $[M–BF_4)]^+$ calcd. 174.1031. Found 174.1032.

Compound 2. 1-(2-pyridyl)-1,2,3-triazole **6** (600 mg, 4.8 mmol) was dissolved in CH_2Cl_2 and stirred 5 min at 0 ºC, then MeOT (1.2 equiv, 4.9 mmol) was added. The mixture was stirred for 20 min. Subsequent addition of Et_2O gave a white precipitate. This precipitate was filtered off and dried, affording compound **2** as a white solid (970 mg, 65%). ^1H NMR (500 MHz, acetone-d_6): δ 9.49 ppm, 9.08 ppm (2 × d, $^3J_{HH}$ = 1.6 Hz, 1H, H_{trz}), 8.75 (dd, $^3J_{HH}$ = 4.8 Hz, $^4J_{HH}$ = 1.0 Hz, 1H, H_{py}), 8.33 (ddd, $^3J_{HH}$ = 8.5 Hz, $^3J_{HH}$ = 7.8 Hz, $^4J_{HH}$ = 1.0 Hz, 1H, H_{py}), 8.27 (td, $^3J_{HH}$ = 8.5 Hz, $^4J_{HH}$ = 1.0 Hz, 1H, H_{py}), 7.82 (ddd, $^3J_{HH}$ = 7.8 Hz, $^3J_{HH}$ = 4.8 Hz, $^4J_{HH}$ = 1.0

Hz, 1H, H_{py}), 4.67 (s, 3H, NCH_3). $^{13}C\{^1H\}$ NMR (125 MHz, acetone–d_6): δ 149.5 (CH_{py}), 146.9 (C_{py}), 141.0 (CH_{py}), 132.9, 127.4 (2 × CH_{trz}), 127.3 (CH_{py}), 115.1 (CH_{py}), 40.1 (N–CH_3). Anal. calcd. for $C_9H_9F_3N_4O_3S$ (310.03): C, 34.84; H, 2.92; N, 18.06; Found: C, 34.71; H, 2.75; N, 17.76. HRMS for $C_8H_9N_4$ $[M–OTf]^+$ calcd. 161.0822. Found: 161.0827.

Complex 3. Compound **1** (100 mg, 0.39 mmol), $[IrCp^*Cl_2]_2$ (155 mg, 0.19 mmol) and Na_2CO_3 (105 mg, 1.0 mmol) were degassed and suspended in degassed and dry dichloroethane (10 mL). The mixture was heated to 60 °C for 16 h. The suspension was filtered trough Celite, and the filtrate layered with Et_2O (150 mL) to form a yellow precipitate. This solid was filtered off, dissolved in MeCN (5 mL) and layered with Et_2O (100 mL) to obtain complex **3** (114 mg, 47%). ^1H NMR (400 MHz, $CDCl_3$): δ 8.95 (dd, $^3J_{HH}$ = 6.0, $^4J_{HH}$ = 1.6 Hz, 1H, H_{py}), 8.14 (dt, $^3J_{HH}$ = 8.0, $^3J_{HH}$ = 7.5 Hz, 1H, H_{py}), 7.92 (d, $^3J_{HH}$ = 2.4 Hz, 1H, H_{imid}), 7.89 (d, $^3J_{HH}$ = 8.0 Hz, 1H, H_{py}), 7.49 (ddd, $^3J_{HH}$ = 7.5 Hz, $^3J_{HH}$ = 6.0 Hz, , $^4J_{HH}$ = 1.6 Hz, 1H, H_{py}), 7.44 (d, $^3J_{HH}$ = 2.4 Hz, 1H, H_{imid}), 4.09 (s, 3H, NCH_3), 3.48, 2.92 (2 × AB, $^2J_{HH}$ = 12.8 Hz, 2H, Ir–CH_2), 1.62 (s, 15H, Cp–CH_3). $^{13}C\{^1H\}$ NMR (125 MHz, $CDCl_3$): δ 159.7 (C_{imid}–Me), 158.1 (CH_{py}), 149.1 (C_{py}), 144.9 (CH_{py}), 128.4 (CH_{py}), 125.1 (CH_{imid}), 121.2 (CH_{imid}), 120.0 (CH_{py}), 90.3 (C_{Cp}), 37.9 (N–CH_3), 11.45 (Cp–*C*H_3), 3.6 (Ir–CH_2). Anal. calcd. for $C_{20}H_{26}N_3ClBF_4Ir$ (622.92): C, 38.56; H, 4.21 N, 6.75. Found: C, 38.82; H, 4.00; N, 6.73.

Complex 4. Compound **1** (100 mg, 0.39 mmol) and $[IrCp^*Cl_2]_2$ (155 mg, 0.19 mmol) were suspended in degassed toluene (8 mL) and stirred at 110 °C for 24 h. A yellow precipitate was formed and the mixture was cooled to RT. The solvent was removed via cannula and the precipitate was dissolved in MeCN and filtered. The filtrate was layered with Et_2O, which induced the formation of a yellow solid that was filtered and dried under vacuum, thus yielding complex **4** (206 mg, 85%). ^1H NMR (500 MHz, CD_3CN): δ 8.74 (dd, $^3J_{HH}$ = 5.6 Hz, $^4J_{HH}$ = 1.0 Hz, 1H, H_{py}), 8.12 (ddd, $^3J_{HH}$ = 8.2 Hz, $^3J_{HH}$ = 7.5 Hz, $^4J_{HH}$ = 1.0 Hz, 1H, H_{py}), 7.99 (d, $^3J_{HH}$ = 8.2 Hz, 1H, H_{py}), 7.50 (ddd, $^3J_{HH}$ = 5.6 Hz, , $^3J_{HH}$ = 7.5 Hz, $^4J_{HH}$ = 1.0 Hz, 1H, H_{py}), 6.89 (s, 1H, CH_{imid}), 3.79 (s, 3H, NCH_3), 2.63 (s, 3H, C_{imid}–CH_3), 1.71 (s, 15H, Cp–CH_3). $^{13}C\{^1H\}$ NMR (100 MHz, CD_3CN): δ 153.4 (CH_{py}), 152.3 (C_{py}), 144.0 (C_{imid}–Ir), 141.5 (CH_{py}), 125.0 (CH_{py}), 121.8 (CH_{imid}), 114.0 (CH_{py}), 90.4 (C_{Cp}), 35.0 (N–CH_3), 12.3 (C_{imid}–*C*H_3), 8.4 (Cp–CH_3). Anal. calcd. for $C_{20}H_{26}N_3BClF_4Ir$ (622.92): C, 38.56; H, 4.21 N, 6.75. Found: C, 38.02; H, 3.83; N, 7.03.

Complex 5. Compound **2** (100 mg, 0.32 mmol) and $[IrCp^*Cl_2]_2$ (123 mg, 0.16 mmol) were suspended in degassed toluene (10 mL) and stirred at 140 °C for 4 h, during which a yellow

precipitate formed. After cooling to RT, the soluble portions were removed via cannula. The residue was dissolved in MeCN and layered with Et_2O (100 mL) to precipitate a yellow solid, which was filtered and dried under vacuum to afford complex **5** (144 mg, 67%). ^{1}H NMR (400 MHz, acetone-*d*$_6$): δ 8.96 (dd, $^3J_{HH}$ = 5.7 Hz, $^4J_{HH}$ = 1.5 Hz, 1H, H_{py}), 8.61 (s, 1H, CH_{trz}), 8.42 (ddd, $^3J_{HH}$ = 8.2 Hz, $^3J_{HH}$ = 7.9 Hz $^4J_{HH}$ = 1.5 Hz, 1H, H_{py}), 8.36 (d, $^3J_{HH}$ = 8.2 Hz, 1H, H_{py}), 7.81 (ddd, $^3J_{HH}$ = 5.7 Hz, $^3J_{HH}$ = 7.9 Hz, $^4J_{HH}$ = 1.5 Hz, 1H, H_{py}), 4.55 (s, 3H, NCH_3), 1.85 (s, 15H, Cp–CH_3). $^{13}C\{^1H\}$ NMR (100 MHz, acetone-*d*$_6$): δ 155.5 (Ir–C_{trz}), 152.4 (CH_{py}), 150.1 (C_{py}), 142.5 (CH_{py}), 133.0 (CH_{trz}), 127.4 (CH_{py}), 114.1 (CH_{py}), 91.4 (C_{Cp}), 39.5 (N–CH_3), 8.3 (Cp–*C*H_3). Anal. calcd. for $C_{19}H_{24}N_4ClF_3IrO_3S$ (673.15): C, 33.90; H, 3.59 N, 8.32. Found: C, 33.93; H, 3.32; N, 8.12**.**

Complex 7. 1-(2-pyridyl)-1,2,3-triazole **6** (20 mg, 0.14 mmol) and $[IrCp^*Cl_2]_2$ (55 mg, 0.07 mmol) were dissolved in CH_2Cl_2 (3 mL) and stirred for 5 min. After that time the mixture was layered with Et_2O (30 mL) and pentane (10 mL), which induced the formation of a yellow solid. The solid was filtered off and dried under vacuum to yield complex **7** (68 mg, 0.13 mmol, 92%). ^{1}H NMR (600 MHz, CD_2Cl_2*,* 253 K) *major rotamer*: δ 8.61 (d, $^3J_{HH}$ = 0.6 Hz, 1H, H_{trz}), 8.50 (ddd, $^3J_{HH}$ = 4.7 Hz, $^4J_{HH}$ = 1.9 Hz, $^5J_{HH}$ = 0.6 Hz, 1H, H_{py}), 8.16 (d, $^3J_{HH}$ = 8.0 Hz, 1H, , H_{py}), 7.95 (ddd, $^3J_{HH}$ = 8.0 Hz, $^3J_{HH}$ = 7.5 Hz, $^4J_{HH}$ = 1.9 Hz, 1H, H_{py}), 7.81 (d, $^3J_{HH}$ = 0.6 Hz, 1H, H_{trz}), 7.38 (ddd, $^3J_{HH}$ = 4.7 Hz, $^3J_{HH}$ = 7.5 Hz, $^4J_{HH}$ = 1.0 Hz, 1H, H_{py}), 1.65 (s, 15H, Cp–CH_3). ^{13}C $\{^1H\}$NMR (150 MHz, CD_2Cl_2*,* 253 K) δ 149.5 (C_{py}), 148.6 (CH_{py}), 139.4 (CH_{py}), 134.2 (CH_{trz}), 123.8 (CH_{py}), 121.2 (CH_{trz}), 113.7 (CH_{py}), 86.5 (C_{Cp}), 8.9 (C_{Cp}–*C*H_3). *Minor rotamer*: δ 8.65 (d, $^3J_{HH}$ = 0.6 Hz, 1H, H_{trz}), 8.54 (ddd, $^3J_{HH}$ = 4.7 Hz, $^4J_{HH}$ = 1.9 Hz, $^5J_{HH}$ = 0.6 Hz, 1H, H_{py}), 8.45 (d, $^1J_{HH}$ = 0.6 Hz, 1H, H_{trz}), 8.07 (d, $^3J_{HH}$ = 8.0 Hz, 1H, H_{py}), 8.02 (ddd, $^3J_{HH}$ = 8.0 Hz, $^3J_{HH}$ = 7.5 Hz, $^4J_{HH}$ = 1.9 Hz, 1H, H_{py}), 7.48 (ddd, $^3J_{HH}$ = 4.7 Hz, $^3J_{HH}$ = 7.5 Hz, $^4J_{HH}$ = 1.0 Hz, 1H, H_{py}), 1.65 (s, 15 H, Cp–CH_3). HRMS for $[M–Cl]^+$ Calc. for $C_{17}H_{21}N_4ClIr$: 509.1084. Found 509.1093. Anal. calcd. for $C_{17}H_{21}N_4Cl_2Ir$ (544.50): C, 37.50; H, 3.89; N, 10.29. Found: C, 37.46; H, 3.66; N, 10.28.

Complex 8: Complex **3** (52.0 mg, 0.090 mmol), AgOTf (46.0 mg, 0.19 mmol) and H_2O (0.02 mL, 1 mmol) were suspended in CH_2Cl_2 (10 mL) and sonicated during 10 min at 40 °C. The mixture was stirred for 14 h and filtered through Celite, and slowly evaporated, which afforded yellow crystals (36 mg, 49%). ^{1}H NMR (500 MHz, D_2O): δ 8.97 (d, $^3J_{HH}$ = 5.6 Hz, 1H, H_{py}), 8.35 (t, $^3J_{HH}$ = 7.9 Hz, 1H, H_{py}), 7.96 (d, $^3J_{HH}$ = 8.3 Hz, 1H, H_{py}), 7.79–7.72 (m, 2H, H_{py}, H_{imid}), 7.45 (s, 1H, H_{imid}), 4.59 (s, 3H, NCH_3), 1.57 (s, 15H, Cp–CH_3). $^{13}C\{^1H\}$ NMR (125 MHz, $CDCl_3$): δ 154.4 (C_{imid}), 153.5 (CH_{py}) 145.7 (C_{py}), 142.1 (CH_{py}), 126.2 (CH_{py}),

121.4 (CH_{imid}), 117.3 (CH_{imid} and CH_{py}), 87.0 (C_{Cp}), 34.1 (N–CH_3), 7.2 (Cp–*C*H_3), 0.1 (CH_2). Anal. calcd. for $C_{21}H_{28}N_3F_6IrO_7S_2$ (840.80) × H_2O: C, 30.99; H, 3.59; N, 5.16. Found: C, 30.88; H, 3.31; N, 4.97.

Complex 9: The title compound was prepared according to the procedure described for **8**, starting from compound **4** (100.0 mg, 0.16 mmol) and AgOTf (45.0 mg, 0.17 mmol). Yield: 107 mg (82%). ^{1}H NMR (500 MHz, D_2O); δ 8.95 (d, $^3J_{HH}$ = 5.5 Hz, 1H, H_{py}), 8.20 (t, $^3J_{HH}$ = 8.6 Hz, 1H, H_{py}), 8.07 (d, $^3J_{HH}$ = 8.6 Hz, 1H, H_{py}), 7.59 (t, $^3J_{HH}$ = 6.6 Hz, 1H, H_{py}), 3.81 (s, 3H, NCH_3), 2.95 (s, 3H, C_{imid}–CH_3) 1.67 (s, 15H, Cp–CH_3). $^{13}C\{^1H\}$ NMR (125 MHz, $CDCl_3$): δ 152.8 (CH_{py}), 144.3 (C_{imid}), 143.0 (CH_{py}), 142.7 (C_{py}), 125.6 (CH_{py}), 123.5 (CH_{imid}), 114.3 (CH_{py}), 89.9 (C_{Cp}), 34.7 (N–*C*H_3), 11.8 (C_{imid}–*C*H_3), 8.2 (Cp–*C*H_3). Anal. calcd. for $C_{22}H_{28}N_3F_6IrO_7S_2$ (816.81): C, 32.35; H, 3.46; N, 5.14. Found: C, 32.83; H, 3.69; N, 4.65.

Complex 10: The title compound was prepared according to the procedure described for **8**, starting from compound **5** (70.0 mg, 0.10 mmol) and AgOTf (35.0 mg, 0.15 mmol), to give complex **10** (49 mg, 59%). ^{1}H NMR (500 MHz, D_2O): δ 8.81 (d, $^3J_{HH}$ = 5.6 Hz, 1H, H_{py}), 8.36 (s, 1H, H_{trz}), 8.25–8.17 (m, 2H, H_{py}), 7.81 (t, $^3J_{HH}$ = 6.5 Hz, 1H, H_{py}), 4.28 (s, 3H, NCH_3), 1.62 (s, 15H, Cp–CH_3). $^{13}C\{^1H\}$ NMR (125 MHz, $CDCl_3$): δ 154.2 (Ir–C_{trz}), 151.7 (CH_{py}), 150.5 (C_{py}), 133.3 (CH_{trz}), 127.8 (CH_{py}), 114.7 (CH_{py}), 90.7 (C_{Cp}), 39.5 (NCH_3), 8.2 (Cp–*C*H_3). Anal. calcd. for $C_{20}H_{25}N_4F_6IrO_7S_2$ (803.77): C, 29.89; H, 3.14; N, 6.97. Found: C, 29.73; H, 3.04; N, 6.78.

General procedure for hydrosilylation. In a typical procedure, acetophenone (60 μL, 0.5 mmol) was added to a solution of CD_2Cl_2 (1 mL) containing the catalyst (5 μmol) and stirred for 5 min. Triethylsilane (160 μL, 1.0 mmol) was added and the catalysis was monitored by transferring aliquots (50 μL) of the reaction mixture to an NMR tube containing $CDCl_3$ (0.6 mL) and subsequent ^{1}H NMR spectroscopic analysis.

General procedure for the oxidation of silanes. In a typical procedure, phenylsilane (190 μL, 1.0 mmol) was added to a solution of CD_2Cl_2 (1 mL) containing the catalyst (5 μmol). The catalysis was monitored by transferring aliquots (50 μL) of the reaction mixture to an NMR tube containing $CDCl_3$ (0.6 mL) and subsequent ^{1}H NMR spectroscopic analysis.

General procedure for water oxidation experiments. In a typical procedure, a solution of the complex (1 mL, see Fig. 5 for final catalyst concentrations) was added to a sealed vial containing a degassed aqueous solution of CAN (10 mL, 0.8 M, 8.0 mmol) The resulting

pressure increase was monitored via manometry. End points were verified by gas chromatography and corrected for contamination.[27a]

Crystallographic details. Crystal data for complexes **3**, **4**, **5**, **7**, **8**, **9**, and **10** were collected by using an Agilent Technologies SuperNova A diffractometer fitted with an Atlas detector using Mo-K_α radiation (0.71073 Å). A complete dataset was collected, assuming that the Friedel pairs are not equivalent. An analytical numeric absorption correction was performed.[40] The structures were solved by direct methods using SHELXS-97[41] and refined by full-matrix least-squares fitting on F^2 for all data using SHELXL-97.[41] Hydrogen atoms were added at calculated positions and refined by using a riding model. Their isotropic temperature factors were fixed to 1.2 times (1.5 times for methyl groups) the equivalent isotropic displacement parameters of the carbon atom the H-atom is attached to. Anisotropic thermal displacement parameters were used for all nonhydrogen atoms. Crystallographic details are compiled in the supporting information (Tables S2-S8). CCDC numbers 1018206–1018212 contain the supplementary crystallographic data for this paper. These data can be obtained free of charge from the Cambridge Crystallographic Data Centre via www.ccdc.cam.ac.uk/data_request/cif.

Supporting Information Available. Detailed water oxidation data, time-conversion profile for water oxidation and hydrosilylation under high turnover conditions, and X-ray crystal data in CIF format for all structures reported in this paper.

Acknowledgements. We thank Dr. Y. Ortin for technical assistance. This work was financial supported by the European Research Council (ERC CoG 615653), the National Science Foundation (CHE-1362629), and SFI through the Synthesis and Solid State Pharmaceutical Research Centre (SSPC, 12/RC/2275).

References

[1] a) According to the IUPAC Golden Book, mesoionic compounds are “Dipolar five-(possibly six-) membered heterocyclic compounds in which both the negative and the positive charge are delocalized, for which a totally covalent structure cannot be written, and which cannot be represented satisfactorily by any one polar structure. The formal positive charge is associated with the ring atoms, and the formal negative charge is associated with ring atoms or an exocyclic nitrogen or chalcogen atom.

Mesoionic compounds are a subclass of betains." IUPAC. Compendium of Chemical Terminology, 2nd ed. (the "Gold Book") compiled by McNaught AD and Wilkinson A. Blackwell Oxford, UK: Scientific Publications; 1997. See also: b) S. Araki, Y. Wanibe, F. Uno, A. Morikawa, K. Yamamoto, K. Chiba, Y. Butsugan, *Chem. Ber.* **1993**, *12*, 1149–1155.

[2] a) P. L. Arnold, J. Pearson, *Coord. Chem. Rev.* **2007**, *251*, 596–609. b) M. Albrecht, *Chem. Commun.* **2008**, 3601–3610. c) O. Schuster, L. Yang, H. Raubenheimer, M. Albrecht, *Chem. Rev.* **2009**, *109*, 3445–3478. d) R. H. Crabtree, *Coord. Chem. Rev.* **2013**, *257*, 755–766.

[3] For selected reviews on NHCs: a) D. Bourissou, O. Guerret, F. P. Gabbai, G. Bertrand, *Chem. Rev.* **2000**, *100*, 39–92. b) F. E. Hahn, M. C. Jahnke, *Angew. Chem. Int. Ed.* **2008**, *47*, 3122–3172. c) A. J. Arduengo, G. Bertrand, *Chem. Rev.* **2009**, *109*, 3209–3210 (thematic issue). d) M. Melaimi, M. Soleilhavoup, G. Bertrand, *Angew. Chem. Int. Ed.* **2010**, *49*, 8810–8849. e) F. Glorius (Ed.), *N-heterocyclic carbenes in transition-metal catalysis*, (Topics in Organometallic Chemistry, Springer, Berlin) 2007. f) C. S. J. Cazin (Ed.), *N-heterocyclic carbenes in transition metal catalysis and organocatalysis*, (Springer, Berlin, Germany), 2011. g) S. Diez-Gonzalez (Ed.), *N-heterocyclic carbenes; From laboratory curiosities to efficient synthetic tools* (RSC Catalysis Series, Cambridge, UK), 2011.

[4] A. Krüger, M. Albrecht, *Aust. J. Chem.* **2011**, *64*, 1113–1117.

[5] a) D. Bacciu, K. J. Cavell, I. A. Fallis, L. Ooi, *Angew. Chem. Int. Ed.* **2005**, *44*, 5282–5284. b) D. Canseco-Gonzalez, A. Gniewek, M. Szulmanowicz, H. Müller-Bunz, A. Trceziak, M. Albrecht, *Chem. Eur. J.* **2012**, *18*, 6055–6062. c) D. Canseco-Gonzalez, A. Petronilho, H. Müller-Bunz, K. Ohmatsu, T. Ooi, M. Albrecht, *J. Am. Chem. Soc.* **2013**, *135*, 13193–13203.

[6] a) S. Gründemann, A. Kovacevic, M. Albrecht, J. W. Faller, R. H. Crabtree, *J. Am. Chem. Soc.* **2002**, *124*, 10473–10481. b) H. Lebel, M. K. Janes, A. B. Charette, S. P. Nolan, *J. Am. Chem. Soc.* **2004**, *126*, 5046–5047. c) J. Schütz, E. Herdtweck, W. A. Herrmann, *Organometallics* **2004**, *23*, 6084–6086.

[7] a) E. Kluser, A. Neels, M. Albrecht, *Chem. Commun.* **2006**, 4495–4497. b) Y. Han, H. V. Huynh, *Chem. Commun.* **2007**, 1089–1091.

[8] a) V. Lavallo, C. A. Dyker, B. Donnadieu, G. Bertrand, *Angew. Chem. Int. Ed.* **2008**, *47*, 5411–5414. b) E. Aldeco-Perez, A. J. Rosenthal, B. Donnadieu, P. Parameswaran, G. Frenking, G. Bertrand, *Science* **2009**, *326*, 556–559.

[9] a) X. Hu, I. Castro-Rodriguez, K. A. Meyer, *Organometallics* **2003**, *22*, 3016–3018. b) A. A. Danopoulos, N. Tsoureas, J. A. Wright, M. E. Light, *Organometallics* **2004**, *23*, 166–168. c) N. Stylianides, A. A. Danopoulos, N. Tsoureas, *J. Organomet. Chem.* **2005**, *690*, 5948–5958. d) C. E. Ellul, M. F. Mahon, O. Saker, M. K. Whittlesey, *Angew. Chem. Int. Ed.* **2007**, *46*, 6343–6345.

[10] a) A. R. Chianese, A. Kovacevic, B. M. Zeglis, J. W. Faller, R. H. Crabtree, *Organometallics* **2004**, *23*, 2461–2468. b) M. Heckenroth, E. Kluser, A. Neels, M. Albrecht, *Angew. Chem. Int. Ed.* **2007**, *46*, 6293–6296.

[11] a) A. R. Chianese, B. M. Zeglis, R. H. Crabtree, *Chem. Commun.* **2004**, 2176–2177. b) M. Viciano, M. Feliz, R. Corberan, J. A. Mata, E. Clot, E. Peris, *Organometallics,* **2007**, *26*, 5304–5314. c) C. Segarra, E. Mas-Marza, J. A. Mata, E. Peris, *Organometallics* **2012**, *31*, 5169–5176. d) C. Segarra, E. Mas-Marza, M. Benitez, J. A. Mata, E. Peris, *Angew. Chem. Int. Ed.* **2012**, *51*, 10841–10845.

[12] a) P. Mathew, A. Neels, M. Albrecht, *J. Am. Chem. Soc*. **2008**, *130*, 13534–13535. b) G. Guisado-Barrios, J. Bouffard, B. Donnadieu, G. Bertrand, *Angew. Chem. Int. Ed.* **2010**, *49*, 4759–4762. For a review, see: c) K. F. Donnelly, A. Petronilho, M. Albrecht, *Chem. Commun.* **2013**, *49*, 1145–1159.

[13] a) For an intriguing reaction that produces complexes from both $C(sp^2)$–H and $C(sp^3)$–H bond activation, see ref 11b. See also b) R. Lalrempuia, N. D. McDaniel, H. Müller-Bunz, S. Bernhard, M. Albrecht, *Angew. Chem. Int. Ed.* **2010**, *49*, 9765–9768.

[14] a) S. T. Handy, M. Okello, *J. Org. Chem.* **2005**, *70*, 1915–1918. b) A. Fürstner, M. Alcarazo, R. Goddard C. W. Lehmann, *Angew. Chem. Int. Ed*. **2008**, *47*, 3210–3214. c) G. Song, X. Li, Z. Song, J. Zhao, Zhang, H. *Chem. Eur. J.* **2009**, 15, 5535–5544. d) S. Sowmiah, V. Srinivasadesikan, M. C. Tseng, Y. H. Chu, *Molecules*, **2009**, *14*, 3780–3813. e) O. Hollóczki, L. Nyulászi, *Org. Biomol. Chem.* **2011**, *9*, 2634–2640.

[15] a) D. L. Davies, S. M. A. Donald, S. A. Macgregor, *J. Am. Chem. Soc.* **2005**, *127*, 13754–13755. b) D. L. Davies, S. M. A. Donald, O. Al-Duaij, J. Fawcett, C. Little, S. A. Macgregor, *Organometallics* **2006**, *25*, 5976–5978. c) S. I. Gorelsky, D. Lapointe, K. Fagnou, *J. Am. Chem. Soc*. **2008**, *130*, 10848–10849. d) D. Balcells, E. Clot, O. Eisenstein, *Chem. Rev*. **2010**, *110*, 749–823.

[16] M. Albrecht, *Chem. Rev* **2009**, 110, 576–623.

[17] a) G. Song, X. Wang, Y. Li, X. Li, *Organometallics* **2008**, *27*, 1187–1192. b) J. Wolf, A. Labande, J.-C. Daran, R. Poli, *Eur. J. Inorg. Chem*. **2008**, 3024–3030.

[18] a) Y. Tulchinsky, M. Iron, M. Botoshansky, M. Gandelman, *Nat. Chem*. **2011**, *3*, 525–531. b) Y. Tulchinsky, S. Kozuch, P. Saha, M. Botoshansky, L J. W. Shimon, M. Gandelman, *Chem. Sci*. **2014**, *5*, 1305–1311.

[19] B. Butschke, H. Schwarz, *Chem. Sci.* **2012**, *3*, 308–326

[20] a) A. Petronilho, M. Rahman, J. A. Woods, H. Al-Sayyed, H.Müller-Bunz, J. M. D. MacElroy, S. Bernhard, M. Albrecht, *Dalton Trans.* **2012**, *41*, 13074–13080. b) J. A. Woods, R. Lalrempuia, A. Petronilho, N. D. McDaniel, H. Müller-Bunz, M. Albrecht, S. Bernhard, *Energy Environ. Sci.* **2014**, *7*, 2316–2328.

[21] In aqueous media, partial Cl^- to OH_2 ligand exchange is observed; this equilibrium is shifted completely to the chloro complex in the presence of Cl^- ions as provided by

HCl. For a detailed discussion of ligand exchange reactions and pH dependent oxidation processes, see: A. Petronilho, A. Llobet, M. Albrecht, *manuscript submitted to Inorg. Chem* (see also uploaded document ic-2014-01894u for review purposes only).

[22] About 25% degradation was detected after 12 h based on the integration of a newly formed product with chemical shifts in a similar area.

[23] a) S. W. Bird, *Tetrahedron* **1996**, *52*, 9945–9952. b) S. I. Kotelevskii, O. V. Prezhdo, *Tetrahedron* **2001**, *57*, 5715–5729.

[24] a) A. Krüger, A. Neels, M. Albrecht, *Chem. Commun.* **2010**, *46*, 315–317. b) A. Krüger M. Albrecht *Chem. Eur. J.* **2012**, *18*, 652–658.

[25] a) B. K. Keitz, J. Bouffard, G. Bertrand, R. H. Grubbs, *J. Am. Chem. Soc*. **2011**, *133*, 8498–8501. b) J. Bouffard, B. K. Keitz, R. Tonner, G. Guisado-Barrios, G. Frenking, R. H. Grubbs, G. Bertrand, *Organometallics* **2011**, *30*, 2617–2627. c) G. Guisado-Barrios, J. Bouffard, B. Donnadieu, G. Bertrand, *Organometallics* **2011**, *30*, 6017–6021.

[26] R. A. Periana, D. J. Taube, S. Gamble, H. Taube, T. Satoh, H. Fujii, *Science* **1998**, *280*, 560–564

[27] a) N. D. McDaniel, F. J. Coughlin, L. L. Tinker, S. Bernhard, *J. Am. Chem. Soc.* **2008**, *130*, 210–217. b) For a review on iridium water oxidation catalysts, see: J. A. Woods, S. Bernhard, M. Albrecht, in *Molecular Water Oxidation Catalysis,* Llobet, A. (Ed.); Wiley: Chichester (UK), 2014, p. 113–133.

[28] A. R. Parent, R. H. Crabtree, G. W. Brudvig, *Chem. Soc. Rev.* **2012**, *42*, 2247–2252.

[29] a) The methylene group in complex **3** may be more vulnerable to oxidative degradation. In related pyridinium derived ylide complexes, complex degradation has been proposed due to the appearance of $^{13}CO_2$ when starting from the precursor that was isotopically labelled at the ylidic position. For details see: reference 13b and b) D. B. Grotjahn, D. B. Brown, J. K. Martin, D. C. Marelius, M.-C. Abadjian, H. N. Tran, G. Kalyuzhny, K. S. Vecchio, Z. G. Specht, S. A. Cortes-Llamas, V. Miranda-Soto, C. van Niekerk, C. E. Moore, A. L. Rheingold, *J. Am. Chem. Soc.* **2011**, *133*, 19024–19027.

[30] a) A. Savini, G. Bellachioma, G. Ciancaleoni, C. Zuccaccia, D. Zuccaccia, A. Macchioni, *Chem. Commun.* **2010**, *46*, 9218–9219. b) J. D. Blakemore, N. D. Schley, D. Balcells, J. F. Hull, G. W. Olack, C. D. Incarvito, O. Eisenstein, G. W. Brudvig, R. H. Crabtree, *J. Am. Chem. Soc.* **2010**, *132*, 16017–16029. c) A. Bucci, A. Savini, L. Rocchigiani, C. Zuccaccia, S. Rizzato, A. Albinati, A. Llobet, A. Macchioni, *Organometallics*, **2012**, 31, 8071–8074.

[31] M. Heckenroth, A. Neels, M. G. Garnier, P. Aebi, A. W. Ehlers, M. Albrecht, *Chem. Eur. J.* **2009,** *15*, 9375–9386.

[32] a) S. Romain, L. Vigara, A. Llobet, *Acc. Chem. Res.* **2009**, *42*, 1944–1953. b) J. F. Hull, D. Balcells, J. D. Blakemore, C. D. Incarvito, O. Eisenstein, G. W. Brudvig, R. H. Crabtree, *J. Am. Chem. Soc.* **2009**, *131*, 8730–8731. c) T. P. Brewster, J. D. Blakemore, N. D. Schley, C. D. Incarvito, N. Hazari, G. W. Brudvig, R. H. Crabtree, *Organometallics* **2011**, *30*, 965–973.

[33] a) H. Junge, N. Marquet, A. Kammer, S. Denurra, M. Bauer, S. Wohlrab, F. Gärtner, M.-M. Pohl, A. Spannenberg, S. Gladiali, M. Beller, *Chem. Eur. J.* **2012**, *18*, 12749–12758. b) A. Savini, A. Bucci, G. Bellachioma, L. Rocchigiani, C. Zuccaccia, A. Llobet, A. Macchioni, *Chem. Eur. J.* **2014**, *20*, 690–697.

[34] K. Riener, M. P. Högerl, P. Gigler, F. E. Kühn, *ACS Catal*. **2012**, *2*, 613–621.

[35] a) A. R. Chianese, R. H. Crabtree, *Organometallics* **2005**, *24*, 4432–4436. b) T. Chen, X. G. Liu, M. Shi, *Tetrahedron*, **2007**, *63*, 4874–4880. c) A. R. Chianese, A. Mo, D. Datta, *Organometallics* **2009**, *28*, 465–472. d) For a review on hydrosilylation catalysis, see: (a) S. Diez-Gonzalez, S. P. Nolan, *Org. Prep. Proc. Int.* **2007**, *39*, 523–559.

[36] S. Park, M. Brookhart, *Organometallics* **2010**, *29*, 6057–6064.

[37] a) J. John, E. Gravel, A. Hagège, H. Li, T. Gacoin, E. Doris, *Angew. Chem. Int. Ed.* **2011**, *50*, 7533–7536. b) B. P. S. Chauhan, A. Sarkar, M. Chauhan, A. Roka, *Appl. Organometal. Chem.* **2009**, *23*, 385–390. c) T. J. Kistenmacher, M. Ross, L. K. Frevel, *J. Appl. Cryst.* **1978**, *11*, 670–671.

[38] a) F. Uhlig, H. C. Marsmann, *^{29}Si NMR Some practical aspects*. Gelest, Inc. (2008). b) P. J. Launer, *Infrared analysis of organosilicon compounds: spectra-structure correlations* in Silicone Compounds Register and Review (Ed. Petrarch Systems Inc.), 1987, p.100.

[39] J. M. Keith, *J. Org. Chem.* **2010**, *75*, 2722–2725.

[40] R. C. Clark J. S. Reid, *Acta Crystallogr.* **1995**, *A51*, 887–897.

[41] G. M. Sheldrick, *Acta Crystallogr.* **2008**, *A64*, 112–122.

Figure for ToC entry only

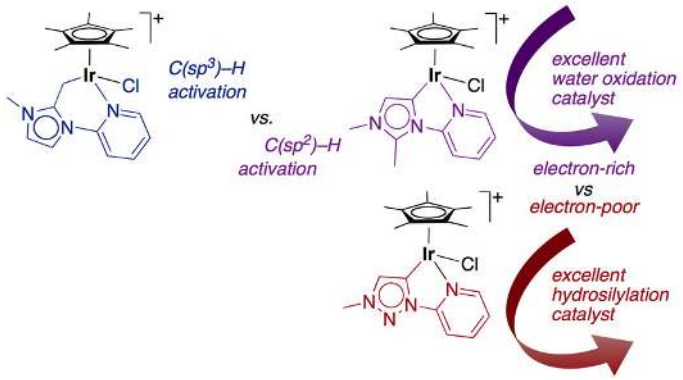

Selective C(sp^2)–H activation of pyridyl-imidazolium salts or of pyridyl-triazolium salts affords isostructural iridium(III) complexes comprised of a mesoionic C-donor ligand. Despite the similar mesoionic character, the behavior of the ligands (e.g. in H/D isotope exchange reactions) and of the complexes (in oxidation catalysis) is distinctly different.